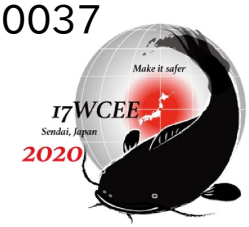

17th World Conference on Earthquake Engineering, 17WCEE
Sendai, Japan - September 13th to 18th 2020

PUNCHING SHEAR FAILURE OF FLAT SLAB STRUCTURE USING STEEL COLUMNS WITH STEEL CAPITALS IN RC SLABS

Y. Yamashita[(1)], Y. Ohta[(2)]

[(1)] *Group Leader, Design Department, Osaka Main Office, Takenaka Corporation, yamashita.yasuhiko@takenaka.co.jp*
[(2)] *General Manager, Structural Engineering Department, R & D Institute, Takenaka Corporation, ohta.yoshihiro@takenaka.co.jp*

Abstract

Flat slab structures and flat plate structures are advantageous in having a high degree of freedom to use indoor spaces because of beamless structures. This paper describes a new construction method using a flat-slab mixed structure with steel capitals in RC slabs. Its distinctive feature is the columns made of small diameter steel round bars instead of RC generally applied. In addition, steel capitals in RC slabs which replace the conventional RC drop panels and capitals will enable the building to provide a space of high quality with unobstructedness as well as flexibility for all designers.

The purpose of this research was to experimentally grasp such performance as punching failure strength, which was considered to be the most important performance of the structure proposed in this study, and the strength and deformation capacity under lateral load. Furthermore, this paper discusses the serviceability limits by observing the residual crack widths of the specimens because particularly in this type of structure the decrease in the rigidity of RC slabs due to cracking significantly affects the properties of the structure.

The following conclusions were obtained from this study:

1) The ultimate vertical force can be calculated with a safety factor of about 10% by using the AIJ standard for RC structures when only the vertical force is transmitted if the circumference of a circle calculated by adding the effective depth of RC slab to the capital plate diameter is deemed to be the critical section for shear in RC slab.

2) It was confirmed from the observation of the crack widths that there was no problem with the usability of RC slabs under sustained loading if the long-term allowable load was set to about 1/3 of the ultimate vertical force when only the vertical force was transmitted.

3) When about 1/3 of the ultimate vertical force for the inner columns and 1/6 for the outer column were applied to RC slabs, none of the lateral loading test specimens including the inner and outer columns in any of the loading directions showed any decrease in resistance to lateral forces until the story drift angle ("R") became 20×10^{-3} rad, which demonstrated their high deformation capacity.

4) Whereas the initial lateral stiffness of the inner and outer column specimens was almost equal when force was applied in a positive direction, the initial lateral stiffness of the outer column with force applied in a negative direction was about a half of the values indicated when force was applied in a positive direction. Furthermore, as the story drift angle increased, the lateral stiffness further reduced due to the damage of RC slabs. We also confirmed that the stiffness of all the specimens at the story drift angle $R=40\times10^{-3}$ rad was about 10 to 20 % of the initial stiffness.

5) The result of our observation of the residual crack widths at the story drift angle often used in the Japanese design criteria for large earthquakes ($R=10\times10^{-3}$ rad) assured us that this structure was highly usable.

6) We also verified that the correlation equation for the shear strength around column capitals was established as $V_u/V_O + M_{max}/M_O \geq 1.0$ according to the AIJ standard for using RC columns when a punching shear failure occurred.

Keywords: flat slab structure; steel column; steel capital; punching shear failure

1. Introduction

A flat slab structure is a structural type with a column capital or a combination of a column capital and a drop panel, in which a slab made of reinforced concrete (hereinafter "RC") is directly integrated into an RC column without any beam between them, as shown in "A" of Fig. 1. On the other hand, a structure without any column capital or drop panel is called a flat plate structure in Japan, distinguished from the former, as shown in "B" of Fig. 1. One of the attractive features of flat slab and flat plate structures is being advantageous in that they have a high degree of freedom to use indoor spaces because of beamless structures. Flat slab structures were first studied by Turner and Maillart in the early twentieth century, and have been widely used afterwards mainly in regions with few earthquakes in Europe and the United States. In recent years, building owners and architects have also recognized the clarity of a flat slab structure, and application of this type of structures to other types of buildings than storages and garages has been on the increase in Japan. Particularly in the structural planning to separate flat slabs from the sufficient seismic elements secured and lightly support them with columns, there are more opportunities to focus on the column sizes.

The new method dealt with in this research employs a flat-slab mixed structure as shown in "C" of Fig. 1, with the following changes made to an RC flat slab structure: (1) an RC column as a vertical supporting member is changed to a steel structure (hereinafter "S structure"); and (2) an RC drop panel is replaced by a steel drop panel (steel capital in Fig. 2 (top)) built in a slab. A steel column is intended to be the most possible slender by using a steel bar or seamless steel tube. Furthermore, the way of vertically supporting a slab in this method simplifies the underside of the slab by using a steel capital in a slab attached on a steel column and achieves elimination of the level difference made by an RC drop panel, like the configuration of a flat plate structure. The feature of a space created by this method is that the aesthetics and sense of tension of structural designers greatly affect their designs as shown in Fig. 2 (bottom) and consequently overwhelming unobstructedness and transparency as well as flexibility can be attained.

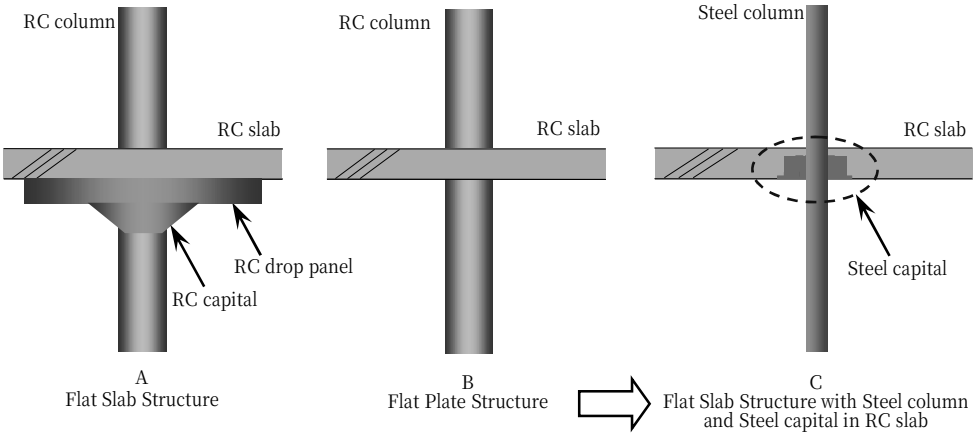

Fig. 1 – Flat slab, flat plate and new type structures

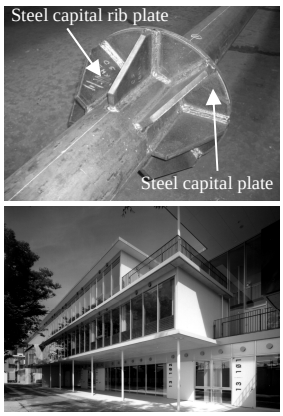

Fig. 2 – Steel capital (top) and building using this new method (bottom)

There were numerous previous studies on flat slab and flat plate structures not only in overseas countries but also in Japan, where such subjects as the review methods for bending, and the calculation methods and design equations for punching failure strength were discussed concerning the stress distribution based on the theory of elasticity as mainly shown by the studies of Kanoh et al. [1-4], the results of which are summarized in the AIJ Standard for Structural Calculation for Reinforced Concrete Structures (hereinafter "RC Standard") [5]. However, most of the previous studies in Japan were performed on RC columns, walls or long columns as vertical supporting members. Few studies have been performed using steel columns. Although there were studies on flat plate structures using CFT columns [6-7], the number of such studies was small. Since occurrence of an extremely large earthquake is predicted in Japan, the authors consider it extremely important to grasp the basic properties of the new construction method towards the realization of a disaster resilient society.

2. Experiment Plan

2.1 Experimental policy

The strength and deformation capacity of flat slab structures vary greatly according to the positions of the columns, such as inner and outer columns, as shown by Fig. 3. The inner columns and outer column referred to here are the names of the column positions defined according to the force application directions. The assumed positions of the later described test specimens are indicated in this diagram. The assumed real building was designed as follows in accordance with the past design performance: 5 stories above the ground, column span measuring 6 meters by 6 meters, 3 meter story height, steel column diameter measuring 210 mm, 300 mm thick slab, specified design concrete strength of Fc27, and the tensile reinforcing-bar quantity at the top of the slabs around the columns: 1.28% (D19@75).The experimental objects were roughly categorized into two types: Those to which only vertical loads were applied ("V" series) and those provided with lateral deformations while a given vertical load assuming sustained loading is applied to the slabs ("H" series).

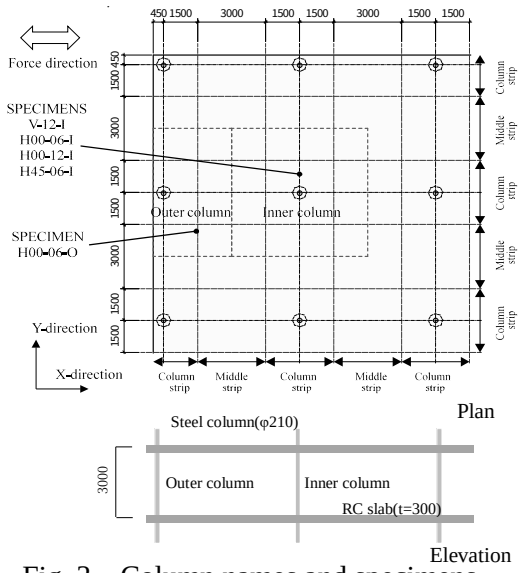

Fig. 3 – Column names and specimens

Table 1 lists the test specimens which are detailed in the following section. The parameters for the specimens were the column positions (inner and outer columns), the rebar content (amount) in the slab, and loads (vertical loads, vertical loads plus X-directional lateral loads, and vertical loads plus oblique lateral loads). The purpose of the specimen V-12-I to which only vertical loads were applied was to confirm the ultimate vertical force when only vertical force was transmitted and to grasp the damage condition of the slab when a load equivalent to a long-term load was applied. As for the specimens H00-06-I, H00-12-I, H45-06-I and H00-06-O with which lateral deformation was provided under given vertical loads, their purpose was to grasp the deformation capacity, the effect of the tensile rebar content (amount) in the slab, the drop in lateral stiffness, the damage condition of the slab, and the punching failure strength against a stress in combination of vertical and lateral loads when an earthquake situation was assumed.

2.2 Test specimens

Table 1 – List of test specimens

Specimen name	Column position		Top reinforcement at column strip (pw)		Bottom reinforcement at column strip (pw)		Top and bottom reinforcement at middle strip (pw)		Force direction		
	Inner	Outer	D6@30 (1.07%)	D6@60 (0.53%)	D6@60 (0.53%)	D6@120 (0.27%)	D6@60 (0.53%)	D6@120 (0.27%)	Vertical	Vertical and lateral in x-direction	Vertical and lateral in xy-direction
V-12-I	○		○		○		○		○		
H00-06-I	○			○		○		○		○	
H00-12-I	○		○		○		○			○	
H45-06-I	○			○		○		○			○
H00-06-O		○		○		○		○		○	

The test specimens were about 1/3 scale models. Figs. 4 to 8 show the configurations of the specimens. The diameter of steel columns and the shape of steel capitals were the same for all the specimens. For the steel types, we used SM490A for steel columns and SS400 for the others. The steel column's length from the upper and lower surface of the slab was 150 mm for V-12-I and 300 mm for the others. The length of the steel columns in the "H" series was cut off at the positions equal to a half of the story height respectively up and down from the slab and set considering the length of the fixture in the experimental equipment.

The diameter of the slab reinforcement was 6 mm (D6), and SD295A was used for the reinforcement type. The amount of the tensile rebars at the upper end of the slab in the column strip is double those in the other areas, like the rebar arrangements of the real building. In the structure proposed by this study, the rebar arrangements in the slab at the upper end and at the lower end respectively interfere with the steel columns and capital ribs, unlike a general RC structure. However, it was assumed in this study that the rebars were kept cut off without any hooks or the like just before the steel columns and capital ribs.

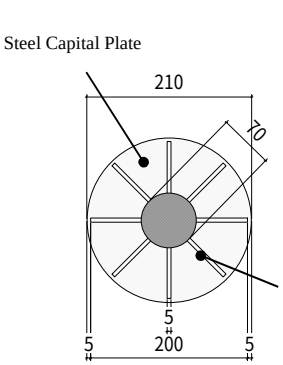

Fig. 4 – Plan of steel capital

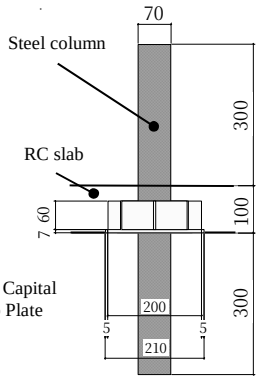

Fig. 5 – Section of steel column and capital (H series)

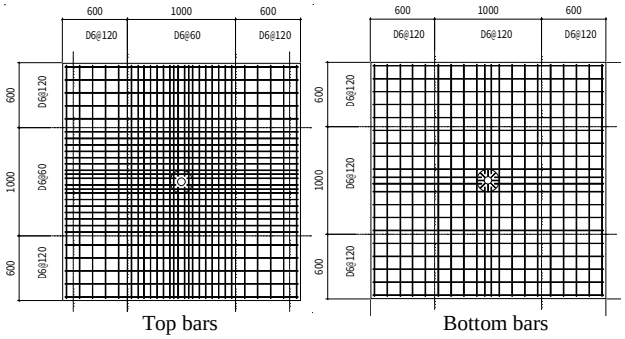

Fig. 6 – Reinforcement of specimen (H00-06-I)

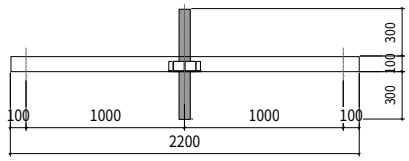

Fig. 7 – Sectional elevation of specimen (H00-06-I)

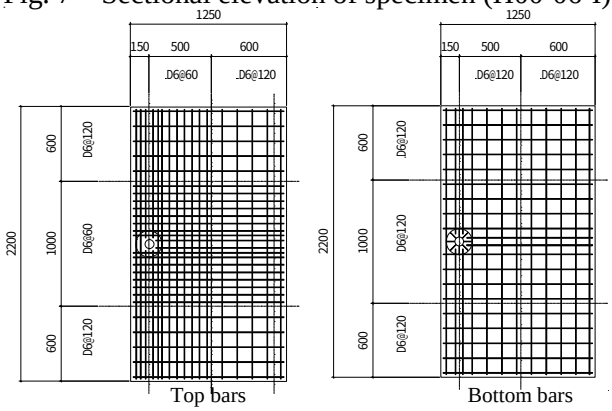

Fig. 8 – Reinforcement of specimen (H00-06-O)

Table 2 – Material characteristics of concrete

Specimens	Compressive strength (N/mm^2)	Young's modulus ($\times 10^4 N/mm^2$)	Tensile strength (N/mm^2)
V-12-I	30.9	2.75	2.62
H-00-06-I	31.6	2.84	2.55
H-00-12-I	31.4	2.86	-
H-45-06-I	31.5	2.84	-
H-00-06-O	31.2	2.84	-

Table 3 – Material characteristics of steel bar

Diameter	Yield stress (N/mm^2)	Young's modulus ($\times 10^5 N/mm^2$)	Tensile strength (N/mm^2)	Elongation (%)
D6	354	1.97	517	21.1
D10	377	1.81	531	17.6

Table 4 – Material characteristics of steel

Places	Yield stress (N/mm^2)	Tensile strength (N/mm^2)	Elongation (%)
Rib plate	396	564	23.9
Capital plate	348	488	26.6
Steel column	613	1018	21.5

2.3 Material test results

Tables 2 to 4 show the material (concrete, rebar and steel) test results of the specimens.

2.4 Vertical loading test program

Fig. 9 shows a setup of a vertical loading device. For the specimens to which only vertical loads were applied, the four sides of the slab were supported by rollers for the distance up to the assumed position of the contraflexure point 1000 mm away from the centre of the steel column. Force was applied as if the lower end of the steel column were pushed up from the bottom, and then the vertical load (N) and the vertical displacement (D) were measured. In designing the specimen V-12-I, we reviewed the punching failure strength and ultimate bending strength of the slab and the ultimate compressive strength of the steel column and planned an occurrence of a punching failure of the slab. The material strength test results shown in Tables 2 to 4 were used for the test program.

To find punching failure strength, applied was an equation using the ultimate vertical force in case where only the vertical forces are transmitted as described in the RC Standard [5]. According to the RC Standard, the punching failure strength (V_O) can be found in the equation (1) below:

$$V_O = \tau_u \cdot A_C \quad (1)$$

$$\tau_u = 0.335 \sqrt{\sigma_b} \quad (2)$$

where τ_u is the direct shear strength of concrete (in N/mm^2); A_C is the sum of the vertical sectional areas (in mm^2) on the sections for punching failure strength calculation; and σ_b is the compressive strength of concrete (in N/mm^2).

According to the equation in the RC Standard, the vertical sectional area (*Ac*) is calculated by adding the effective depth of the slab (*d*) to each side if the RC column is rectangular. On the other hand, since the capital plates of the specimens are circular, the circumference of the circle which is found by adding the effective depth of the slab (*de*) to the diameter of the capital plate is calculated as a section for punching failure strength calculation by means of the equation (3) as shown in Fig. 10.

In the method introduced in this paper, the effective depth of the slab was found by subtracting the capital plate thickness (*tcp*) from the effective depth of the slab (*d*) in the RC Standard.

$$A_C = L_p \cdot d_e \quad (3)$$

$$L_p = (D_{cp} + d_e) \cdot \pi \quad (4)$$

$$d_e = t_S - C - d_S/2 - t_{cp} \quad (5)$$

where L_p is the circumference of the section for punching failure strength calculation (in mm); D_{cp} is the diameter of the capital plate (in mm); d_e is the effective depth of the slab in this method (in mm); t_S is the slab thickness (in mm); C is the covering depth of the top reinforcement (in mm); d_S is the nominal diameter of the slab reinforcement; and t_{cp} is the capital plate thickness (in mm).

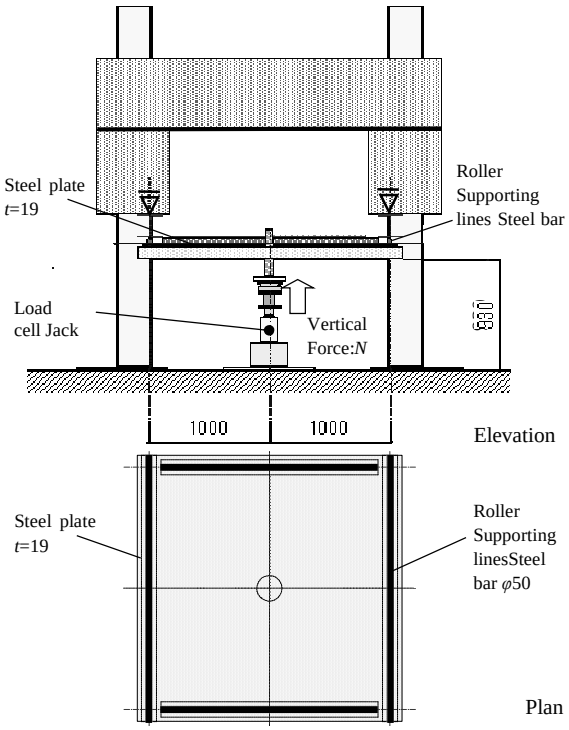

Fig. 9 – Loading setup for vertical load

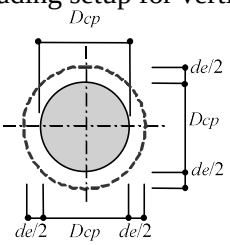

Fig. 10 –Section for calculation of punching failure: *Vo*

Table 5 – Calculation results (V-12-I)

Slab					Column
Punching failure strength				Ultimate bending strength	Ultimate compression strength
τ_u(kN/mm^2)	L_p(mm)	d_e(mm)	V_o(kN)	V_b(kN)	V_c(kN)
1.86	911	80	135.7	326.2	35258

Assuming that a one-directional beam to which a central concentrated load was applied was used for the ultimate bending strength of the slab, it was evaluated as the sum of those in two directions: the X- and Y- directions. The ultimate compressive strength of the steel column was calculated by multiplying the tensile strength by the sectional area due to the shorter column of the specimen. Table 5 shows the calculation results. The strength of the specimen V-12-I was expected to depend upon V_O, the punching failure strength of the slab. The thickness and other specifications of the capital plate and ribbed plate were determined as shown in Figs. 4 and 5 so that the compressive stresses might not exceed the allowable stress for temporary loading on the assumption that they are applied to the capital plate, uniformly distributed by using the calculation results of V_O.

2.5 Lateral loading test program

Fig. 11 shows a setup of a lateral loading device. For the test specimens, the two sides (one side for H00-06-O deemed to be an outer column) of the slab which were perpendicular to the loading direction were supported by the rollers, and the lower ends of the steel columns were supported by pins. Vertical loads were applied to the positions equally away from the centre of a steel column to consider a vertical load stress state, and then lateral loads were applied with the vertical loads kept constant. The lateral load (*Q*), and the story drift angle (*R*) found from the upper and lower lateral displacements of the steel column (δu and δl) were grasped as shown in the diagram. For the lateral displacements δ_u and δ_l, the relative displacements were measured by providing the specimen's slab with reference points. Though the positive and negative loading

directions are shown in the diagram, the positive loads were applied to the outer column specimen in a direction which caused the top of the steel column to fall down to the outer end of the slab. As for the vertical loads, a load equal to one-third of the ultimate vertical force (V_O) transmitted when only the calculated vertical forces were transmitted was considered to be a target, which was applied by vertical loading jacks. The lateral forces were applied with displacements controlled, the positive and negative loads were repeated twice at the story drift angles: 1, 2, 3.33 (1/300), 5, 6, 8, 10, 15, 20, 30 and 40/1000 rad, and then a force was applied up to 1/10 rad in positive loading, which finished the experiment.

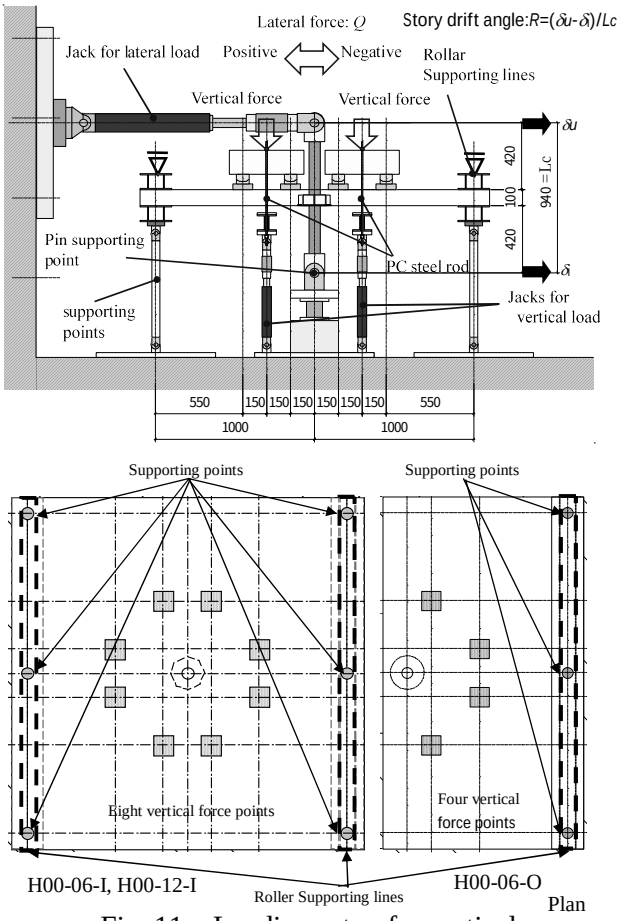

Fig. 11 – Loading setup for vertical and lateral loads

In designing of the lateral loading test specimens, mainly the punching failure strength and ultimate bending strength of the slab in consideration of the vertical load, 1/3 V_O, were compared, and an occurrence of a punching failure was planned. In reviewing the V_O of the outer column, a range equal to three-fourths (3/4) of the circumference of a circle was considered to be a section for punching failure strength calculation in consideration of the outer end. Although the term “punching failure” is used in Sections 2.4 and 2.5 of this paper, we supplement that the failure mechanisms of the two differ because the failure in this section can be considered to be the shear failure caused by the additional shear force accompanying the torsional resistance of the slab on the side and the shear force accompanying the bending of the parts regarded as the front and rear beams unlike the one discussed in the preceding section. The material test results shown in Tables 2 and 3 were used for the calculations. The rebars cut off because of their interferences with the steel columns and capital ribs which are described in Section 2.2 were not considered in the strengths. Besides, a distance to the slab edge is critical for the outer column of a flat slab structure. The distance to the slab edge of the specimen H00-06-O was determined out of consideration so that the anchorage length of the rebars from the inner end of the capital plate might be not less than 40 d. Because there is more than enough bending strength of the steel columns, the study results about it are omitted here.

The equation of the ultimate moment *Mo* (6) transmitted when only the moment was transmitted as described in the RC Standard [5] was applied to the punching failure strength of the slab. In the equation stated in the RC Standard, the effective depth of the slab (*d*) is added to each side to produce a section for the punching failure strength calculation if the RC column is rectangular. However, since the capital plate in the method introduced in this paper is circular, calculation was made by using the inscribed square of the capital plate shown in Fig. 12 as an assumed column. In the equation (7), expression was changed to the product of the number and sectional area of rebars from AIJ equation. To calculate the bending moment caused by the top and bottom reinforcements, the effective depth of the slab was calculated by separating it into the *d* in the RC Standard’s equation and the *de* as a result of subtracting the capital plate thickness from the *d*, in consideration of the reinforcement positions. The *de* was used for the effective depth of the slab in

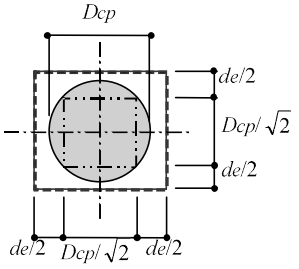

Fig. 12 – Section for calculation of punching failure: *Mo*

the equations (8) and (9). The correlation equation (11) for the punching failure around the columns is shown in the RC Standard. Since the vertical loads for the specimens were designed to be 1/3 V_o, the lateral load in case of a punching failure (Q) was calculated by multiplying the ultimate transmitted moment by 2/3.

$$M_O = M_f + M_S + M_t \tag{6}$$

where M_f is the bending moment transmitted by the bending resistance of the slab on the section for calculation; M_S stands for the bending moment transmitted by the front and rear shear forces on the section for calculation; and M_t stands for the bending moment transmitted by the torsions of the both sides of the section for calculation.

$$M_f = 0.9 \cdot a_t \cdot \sigma_y \cdot d_e \cdot n_t + 0.9 \cdot a_b \cdot \sigma_y \cdot d \cdot n_b \tag{7}$$

$$M_S = \tau_u \cdot (D_{cp}/\sqrt{2} + d_e) \cdot d_e \cdot (D_{cp}/\sqrt{2} + d_e) \tag{8}$$

$$M_t = 6 \cdot \tau_u \cdot {d_e}^2/2 \cdot \{(D_{cp}/\sqrt{2} + d_e) - d_e/3\} \cdot 2 \tag{9}$$

$$d = t_S - C - d_S/2 \tag{10}$$

where a_t is the sectional area of the top reinforcement (in mm^2); a_b is the sectional area of the bottom reinforcement (in mm^2); n_t and n_b respectively stand for the numbers of the top and bottom reinforcements in a section for punching failure strength calculation; and σ_y is the yield strength (in N/mm^2) of the reinforcements. The sectional area of reinforcements for the specimen H45-06-I was calculated by multiplying the sectional area by cos θ to find the effective section.

$$Vu/Vo + Mu/Mo \leqq 1.0 \tag{11}$$

where V_u is the ultimate vertical force (in kN); and M_u is the ultimate transmitted moment (in kN · m).

The ultimate bending strength of the slab was calculated in the equation (12), applying the equation for the ultimate bending strength of the beam which was described in the RC Standard. In case of calculation for the outer column, the tensile reinforcement position was considered according to the loading direction.

$$M_u = 0.9 \cdot a_t \cdot \sigma_y \cdot d_e \cdot {}_{all}n_t + 0.9 \cdot a_b \cdot \sigma_y \cdot d \cdot {}_{all}n_b \tag{12}$$

where ${}_{all}n_t$ and ${}_{all}n_b$ respectively stand for the numbers of the top and bottom reinforcements for the whole section width of the slab. However, the rebars cut off near the steel columns were not considered.

Table 6 shows the calculation results. The strengths of all the specimens were expected to depend upon the punching failure of the slab. However, the negative loading direction of the outer column specimen H00-06-O had a little difference between the punching failure strength and ultimate bending strength of the slab. In the experiment of the outer column type specimen, we could apply only the vertical load of approximately 1/6 (= 0.17) V_o, smaller than the planned 1/3 V_o due to a mistake in operating a vertical loading jack.

Table 6 – Calculation results (H-series)

Specimens	Force direction	Punching failure strength							Ultimate bending strength	Maxiumum lateral force
		V_o (kN)	$1/3V_o$ (kN)	M_f (kN·m)	M_s (kN·m)	M_t (kN·m)	M_o (kN·m)	$2/3M_o$ (kN·m)	M_u (kN·m)	Q (kN)
H00-06-I	Both	137.3	45.8	5.0	7.9	14.6	27.5	18.3	33.8	19.5
H00-12-I	Both	136.8	45.6	6.7	7.8	14.6	29.1	19.4	69.2	20.6
H45-06-I	Both	137.0	45.7	3.6	7.9	14.6	26.0	17.3	31.1	18.4
H00-06-O	Positive	102.3	34.1	3.3	3.9	14.5	21.7	14.4	19.6	15.4
	Negative			2.0	3.9	14.5	20.4	13.6	15.6	14.4

3. Vertical Loading Test

3.1 Results of vertical loading test

Fig. 13 shows the relations between the vertical loads (N) and vertical displacements (D) of the specimen V-12-I. The same graph also shows the 1/3 V_o. The charts in Fig. 14 respectively show the crack propagations

of the upper surface of the slab under the different loads. At [N = 20.6 kN, D = 2.0 mm], an initial crack was formed at a joint with the steel column on the upper surface of the slab of the specimen V-12-I, and then numerous cracks propagated radially. It was confirmed that the area around the steel column on the upper surface of the slab was gently uplifted at [N = 90.7 kN, D = 9.5 mm]. The load reached the maximum value at [N = 154.0 kN, D = 30.2 mm], and the strength abruptly dropped due to a punching failure as shown in Fig. 14 (3). Although no cracks were formed in the lower surface of the slab, the capital plate was recognized to sink into the concrete.

The experimental maximum load was 1.13 times larger than calculated in accordance with the equation in the RC Standard [5], the reason for which is considered to be because the strength equation in the RC Standard does not include the effects of the reinforcements.

3.2 Confirmation of slab's usability under sustained loading

Fig. 15 shows the change of the maximum crack width of the vertical loading test specimen V-12-I to which vertical loads were applied, where the vertical load 45.2 kN was equivalent to the load at one-third of V_O, the calculated punching failure strength of the slab, which was the value set as a target for the long-term allowable load. In the Reference [8], the allowable crack widths, 0.15 mm for the water leakage resistance and 0.50 mm for the deterioration resistance, are described as performance evaluation items. The experimental crack width at 45.2 kN, the vertical load assuming sustained loading, was at maximum 0.06 mm. The width in consideration of the scaling down for the experiment, 0.18 mm, is almost equal to or under the above-mentioned allowable crack widths. Consequently, the slab under sustained loading can be said to be sound as a result of our observation of the crack widths.

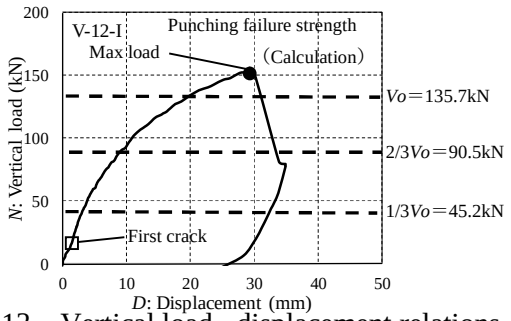

Fig. 13 – Vertical load - displacement relations

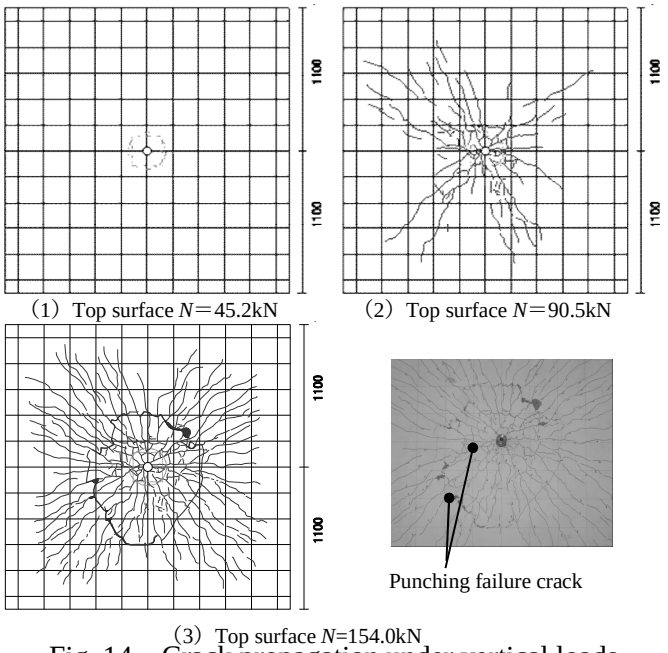

Fig. 14 – Crack propagation under vertical loads

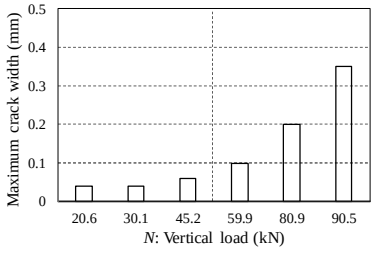

Fig. 15 – Maximum crack width - vertical load relations

4. Lateral Loading Test

4.1 Results of lateral loading test on inner column type specimens

Fig. 16 shows the relations between the lateral loads (Q) and story drift angles (R) of the inner column type specimens. The lateral solid lines in the graphs represent the calculated maximum lateral loads in Table 6. The positive story drift angles along the lateral axis represent those in the positive loading direction in Fig. 11. In case of the specimen H00-06-I, an initial crack was formed in the interface between the upper surface

of the slab and the steel column at [Q = −4.9 kN, R=−1.8×10^{-3} rad]. On the lower surface of the slab, an initial crack was formed in the interface between the slab and the capital plate at [Q = −17.3 kN, R = −8.2 × 10^{-3} rad]. Furthermore, concrete flaking was observed at the interface between the lower surface of the slab and the capital plate at [Q = −26.5 kN, R = −20.1 × 10^{-3} rad]. After the maximum load was reached at [Q = 28.6 kN, R = 20.1 × 10^{-3} rad], crushing of concrete was observed near the steel columns on the upper and lower surfaces of the slab in a cycle of R = 30 × 10^{-3} rad. Sinking of the capital plate into the slab became conspicuous in a cycle of R = 40 × 10^{-3} rad. Uplift of the slab's upper surface and circular cracks were more clearly observed at R = 50.4 × 10^{-3} rad. Fig. 17 shows the cracks on the upper surface of the slab of the specimen H00-06-I at the end of the test. H00-12-I and H45-06-I were slightly later cracked than H00-06-I (on the tops at R=6.0×10^{-3} rad and on the bottoms at R=8.0×10^{-3} rad) and less propagated. However, there ware hardly differences in the maximum strength between them. The maximum strength depended upon a punching failure and exceeded the value calculated in Section 2.5. It was also confirmed that all of the tested specimens showed high deformation capacity up to R=20×10^{-3} rad, without showing any decline in resistance to lateral forces. None of the inner column type specimens had any yielded slab reinforcement.

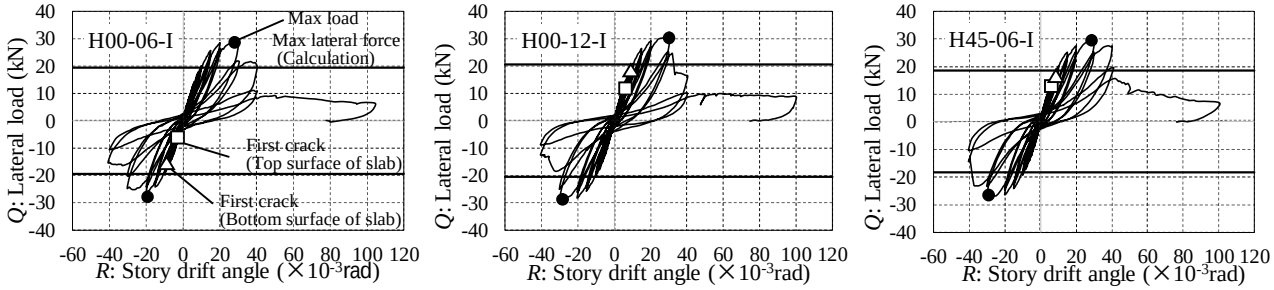

Fig. 16 – Lateral load - lateral drift angle relations of inner columns

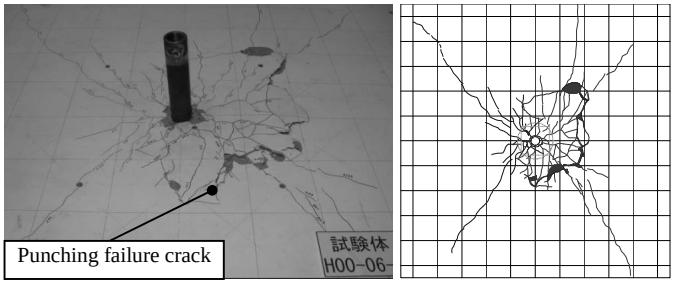

Fig. 17 – Cracked state of slab top surface at end of experiment (H00-06-I)

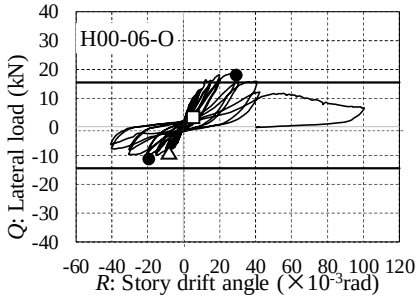

Fig. 18 – Lateral load - lateral drift angle relations

4.2 Results of lateral loading test on outer column type specimen

Fig. 18 shows the relations between the lateral loads (Q) and story drift angles (R) of the outer column type specimen. The vertical loads in the experiment were about 1/6 (= 0.17) V_O, smaller than the planned 1/3 V_O as described in Section 2.5. The positive story drift angles along the lateral axis represent those in the positive loading direction in Fig. 11, which is a direction which caused the upper part of the steel column to fall down to the outer end of the slab. In the specimen H00-06-O, an initial crack was formed in the interface between the upper surface of the slab and the steel column at [Q = 2.7 kN, R = 0.78 × 10^{-3} rad]. On the lower surface of the slab, an initial crack was formed in the interface between the slab and the capital plate at [Q = −7.4 kN, R = −5.1 × 10^{-3} rad]. After the sinking of the capital plate into the slab was observed at [Q = −10.0 kN, R = −15.2 × 10^{-3} rad], the maximum load was reached at

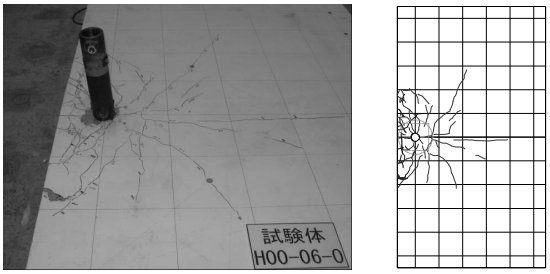

Fig. 19 – Cracked state of slab top surface at end of experiment (H00-06-O)

[Q = 18.3 kN, R = 30.0 × 10^{-3} rad]. Although the uplift of the slab's upper surface became clearer in a cycle of R = 40 × 10^{-3} rad, the circular cracks were not so clear as those of the inner column specimens. Fig. 19 shows the cracks on the upper surfaces of the slab at the end of the test. They were cracked earlier than those of the inner column type specimen H00-06-I. The maximum strength under positive loading was 18.3 kN, which exceeded the calculated value 15.4 kN. However the maximum strength under negative loading was 10.2 kN, which did not reach the calculated value 14.3 kN. Although no crack caused by a clear punching failure was observed on the upper surface of the slab, compared with the inner column specimens as shown in Fig. 19, it can be considered from the post-experiment uplift of the slab's upper surface under positive loading that the maximum strength depended upon a punching failure.

The reason why the maximum strength was under the calculated value is considered because it was assumed in the calculation process that the rebars throughout the whole slab width would yield, which agrees with the decline in the stiffness of the specimen according to the story drift angles as shown in the following section or the changes of their effective widths (lateral stiffness reduction). It was also confirmed that the deformation capacity was as high as those of the inner column specimens, regardless of the loading direction.

4.3 Lateral stiffness

The initial stiffness of all the inner column specimens was almost the same. The same can be said for the secant stiffness up to the maximum strength. On the other hand, the initial stiffness of the outer column specimen under force application in a positive direction was almost the same as those of the inner column specimens. However, the stiffness under force application in a negative direction in which the top of the steel column fell down in a direction opposite to that of the outer end of the slab was 53% of the values under force application in a positive direction.

Fig. 20 shows the ratios of the secant stiffness to the initial stiffness on the assumption that the initial stiffness of each specimen in the first cycle of the experiment is represented by K_0 and the secant stiffness in the following cycles by K. The larger the story drift angle, the lower the lateral stiffness because of such reasons as the damage to the slabs. The stiffness of all the specimens declined to about 10 to 20 % of the initial stiffness at the story drift angle of 40×10^{-3} rad. According to the commentary in the RC Standard, it is described that the stiffness of a flat slab structure abruptly declines due to the cracking started at the low loading stage. We confirmed that the method introduced in this paper has the same tendency.

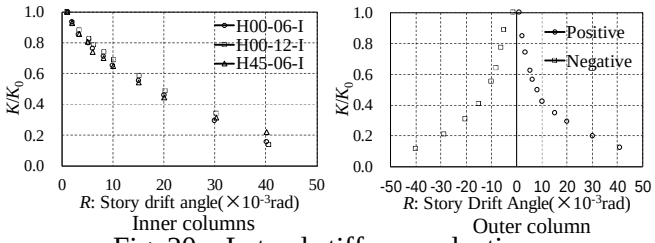

Fig. 20 – Lateral stiffness reductions

4.4 Confirmation of slab's restorability under lateral loading

Fig. 21 shows the changes of the maximum crack widths at the peak story drift angle and the resultant residual crack widths in two cases, where a residual crack width means the crack measured at a zero-load point after experiencing the first maximum deformation angle during two repeated loadings. Compared with the specimen H00-12-I, an initial crack was formed earlier in the specimen H00-06-I with fewer rebars in the column strips around the steel column. Although the crack range was also slightly larger, the maximum crack width was small. Moreover, no excessive vertical deformation of the slab was observed in any specimens at the end of the experiment although Fig. 20 shows that the lateral stiffness decreased to about 60% of the initial stiffness at the story drift angle (R) =10×10^{-3} rad. Both the specimens showed that the

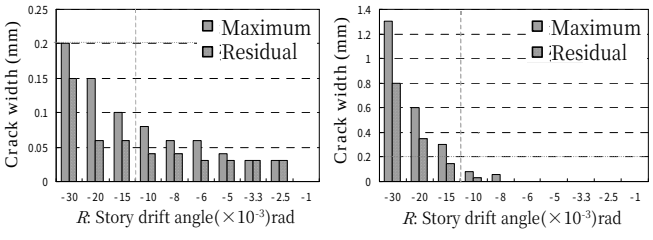

Fig. 21 – Maximum crack width - lateral load relations

residual crack width considering the scaling down for the experiment was 0.18 mm at the story drift angle (R=10×10^{-3} rad) generally often used as the target value in designing against large earthquakes, which was no more than 0.2 mm, a serviceability limit state [9]. Hence, we were able to confirm the restorability of the slabs (the limit state in which the building can be reasonably restored to its original condition) as a result of our observation of the crack widths.

4.5 Punching failure strength

It was confirmed in this experiment that all the specimens of the inner and outer columns showed high deformation capacity without declining in strength until R=20×10^{-3} rad though local damage caused by the bearing around the columns was observed.

Table 7 shows the comparison of the calculated and experimental values of punching failures, where Q_{max} stands for the maximum experimental lateral load; M_{max} is the maximum experimental bending moment; and V_u is the vertical load transmitted to the steel column from the slab at the maximum experimental lateral load, which is the value as found from the balancing of external forces. The reason why the V_u value of the outer column specimen under positive force application differs significantly from the value under negative force application was because of the effect of the variable axial forces. Fig. 22 shows a correlation chart of the experiment results of punching failure around the column capital as shown in the RC Standard [5], in which the relations between V_u / V_O and M_{max} /M_O in this experiment are plotted. The chart indicates that the correlation of V_u / V_O + M_{max} /M_O ≥ 1.0 is established for the specimens H00-06-I, H00-12-I, H45-06-I and H00-06-O which resulted in punching failures (under positive loading) in this experiment. On the other hand, the correlation of V_u /V_O + M_{max} /M_O < 1.0 is established for the specimen H00-06-O which resulted in bending failure (under negative loading). The reason why only the specimen H00-06-O (under negative loading) is away from the line of V_u /V_O + M_{max} /M_O = 1.0 is considered to be because it is affected by the concept of the effective width of the slab in the study of the bending failure strength discussed in Section 4.2. Thus we were able to confirm that the correlation equation for a punching failure as shown in the RC Standard could be applied to a flat slab structure with a steel column and a steel capital built in a slab under the calculation conditions used in this study.

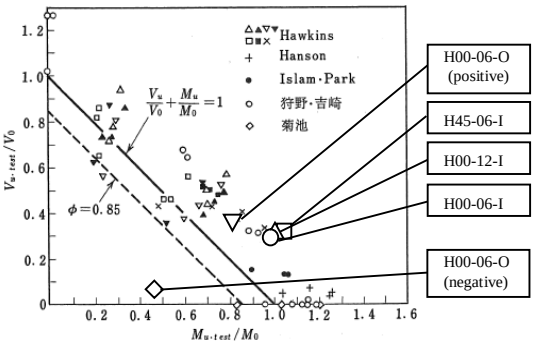

Fig. 22 – V_u/V_O - M_{max}/M_O relations

Table 7 – Comparison of calculated values and experimental values of punching failures

Specimens	Force direction	Calculation			Experiment						
		V_o (kN)	M_o (kN·m)	Q (kN)	V_u (kN)	V_u/V_o	Q_{max} (kN)	$R(\because Q_{max})$ ($\times 10^{-3}$rad)	M_{max} (kN)	M_{max}/M_o	V_u/V_o +M_{max}/M_o
H00-06-I	Both	137.3	27.5	19.5	39.8	0.29	28.6	20.1	26.9	0.98	1.27
H00-12-I	Both	136.8	29.1	20.6	40.9	0.30	31.0	29.2	29.1	1.00	1.30
H45-06-I	Both	137.0	26.0	18.4	41.9	0.31	29.3	28.5	27.5	1.06	1.37
H00-06-O	Positive	102.3	21.7	15.4	34.3	0.34	18.6	27.3	17.5	0.81	1.14
	Negative		20.4	14.4	7.5	0.07	10.2	-20.5	9.6	0.47	0.54

5. Conclusions

The following conclusions were obtained from this study:

1) The ultimate vertical force can be calculated with a safety factor of about 10% by using the AIJ standard for RC structures when only the vertical force is transmitted if the circumference of a circle calculated by adding the effective depth of RC slab (the result of subtracting the capital plate thickness from the effective depth of the RC slab based on the RC standard) to the capital plate diameter is deemed to be the critical section for shear in RC slab.

2) It was confirmed from the observation of the crack widths that there was no problem with the usability of RC slabs under sustained loading if the long-term allowable load was set to about 1/3 of the ultimate vertical force when only the vertical force was transmitted.

3) When about 1/3 of the ultimate vertical force for the inner columns and 1/6 for the outer column were applied to RC slabs, none of the lateral loading test specimens including the inner and outer columns in any of the loading directions showed any decrease in resistance to lateral forces until the story drift angle ("*R*") became 20×10^{-3} rad, which demonstrated their high deformation capacity.

4) Whereas the initial lateral stiffness of the inner and outer column specimens was almost equal when force was applied in a positive direction, the initial lateral stiffness of the outer column with force applied in a negative direction was about a half of the values indicated when force was applied in a positive direction. Furthermore, as the story drift angle increased, the lateral stiffness further reduced due to the damage of RC slabs. We also confirmed that the stiffness of all the specimens at the story drift angle $R=40\times10^{-3}$ rad was about 10 to 20 % of the initial stiffness.

5) The result of our observation of the residual crack widths at the story drift angle often used in the Japanese design criteria for large earthquakes ($R=10\times10^{-3}$ rad) assured us that this structure was highly usable.

6) We also verified that the correlation equation for the shear strength around column capitals was established as $V_u/V_O + M_{max}/M_O \geq 1.0$ according to the AIJ standard for using RC columns when a punching shear failure occurred.

6. Acknowledgements

We hereby express our gratitude to Prof. Yasushi Sanada at Graduate School of Engineering, Osaka University, for his guidance and support in preparing this paper.

7. References

[1] Kanoh Y, Yoshizaki S (Feb. 1980): Tests of Slab-Column Connection Under Repeated Lateral Load (Part 1). *Transactions of the Architectural Institute of Japan*, 288, 39-47 (in Japanese).

[2] Kanoh Y, Yoshizaki S (Jun. 1980): Tests of Slab-Column Connections Transferring Shear and Moment (Part 2). *Transactions of the Architectural Institute of Japan*, 292, 31-39 (in Japanese).

[3] Yoshizaki S, Kanoh Y (Feb. 1981): Study on Strength of Slab-Column Connections (Part 3) Torsion Tests of Connections). *Transactions of the Architectural Institute of Japan*, 300, 41-48 (in Japanese).

[4] Yoshizaki S, Kanoh Y (Nov. 1981): Strength of Slab–Column Connections - Transferring Shear and Moment (Part 4) -. *Transactions of the Architectural Institute of Japan*, 309, 29-40 (in Japanese).

[5] Architectural Institute of Japan (Dec. 2018): *AIJ Standard for Structural Calculation for Reinforced Concrete Structures* (in Japanese).

[6] Satou H, Shimazaki S (Apr. 2005): Lateral Load-Deflection of CFT Column/Flat Plate Joints. *Journal of Structural and Construction Engineering (Transactions of AIJ)*, 590, 145-152 (in Japanese).

[7] Yamaguchi T, Shimazaki S, Satou H (Apr. 2007): An Experimental Study on Vertical Load Resistance of CFT Column-Flat Plate Joints. *Journal of Structural and Construction Engineering (Transactions of AIJ)*, 614, 163-170.

[8] Architectural Institute of Japan (Apr. 2010): *Recommendations for Practice of Crack Control in Reinforced Concrete Buildings (Design and Construction)*, 45-47 (in Japanese).

[9] Architectural Institute of Japan (Jan. 2004): *Guidelines for Performance Evaluation of Earthquake Resistant Reinforced Concrete Buildings (Draft)*, 69-70 (in Japanese).

